Title
Concentric retinitis pigmentosa: clinicopathologic correlations.

Journal
Experimental eye research, 73(4)

ISSN
0014-4835

Authors
Milam, AH
De Castro, EB
Smith, JE
et al.

Publication Date
2001-10-01

DOI
10.1006/exer.2001.1059

Peer reviewed

Exp. Eye Res. (2001) **73**, 493–508
doi:10.1006/exer.2001.1059, available online at http://www.idealibrary.com on IDEAL®

Concentric Retinitis Pigmentosa: Clinicopathologic Correlations

ANN H. MILAM[a]*, ELAINE B. DE CASTRO[a], JULIE E. SMITH[a], WAI-XING TANG[a], SINOJ K. JOHN[a], MICHAEL B. GORIN[b], EDWIN M. STONE[c], GUSTAVO D. AGUIRRE[d] AND SAMUEL G. JACOBSON[a]

[a]*Department of Ophthalmology, Scheie Eye Institute, University of Pennsylvania, Philadelphia, PA 19104, U.S.A.,* [b]*Departments of Ophthalmology and Human Genetics, University of Pittsburgh, Pittsburgh, PA 15213, U.S.A.,* [c]*Department of Ophthalmology and Visual Science, University of Iowa Hospital and Clinics, Iowa City, IA 52243, U.S.A. and* [d]*James A. Baker Institute for Animal Health, College of Veterinary Medicine, Cornell University, Ithaca, New York, NY 14853, U.S.A.*

(*Received St. Louis 10 May 2001 and accepted in revised form 15 June 2001*)

Progressive concentric (centripetal) loss of vision is one pattern of visual field loss in retinitis pigmentosa. This study provides the first clinicopathologic correlations for this form of retinitis pigmentosa. A family with autosomal dominant concentric retinitis pigmentosa was examined clinically and with visual function tests. A post-mortem eye of an affected 94 year old family member was processed for histopathology and immunocytochemistry with retinal cell specific antibodies. Unrelated simplex/multiplex patients with concentric retinitis pigmentosa were also examined. Affected family members of the eye donor and patients from the other families had prominent peripheral pigmentary retinopathy with more normal appearing central retina, good visual acuity, concentric field loss, normal or near normal rod and cone sensitivity within the preserved visual field, and reduced rod and cone electroretinograms. The eye donor, at age 90, had good acuity and function in a central island. Grossly, the central region of the donor retina appeared thinned but otherwise normal, while the far periphery contained heavy bone spicule pigment. Microscopically the central retina showed photoreceptor outer segment shortening and some photoreceptor cell loss. The mid periphery had a sharp line of demarcation where more central photoreceptors were near normal except for very short outer segments and peripheral photoreceptors were absent. Rods and cones showed abrupt loss of outer segments and cell death at this interface. It is concluded that concentric retinitis pigmentosa is a rare but recognizable phenotype with slowly progressive photoreceptor death from the far periphery toward the central retina. The disease is retina-wide but shows regional variation in severity of degeneration; photoreceptor death is severe in the peripheral retina with an abrupt edge between viable and degenerate photoreceptors. Peripheral to central gradients of unknown retinal molecule(s) may be defective or modify photoreceptor degeneration in concentric retinitis pigmentosa.

Key words: retinitis pigmentosa; human retinal disease; rods; cones; histopathology; perimetry; electroretinography; optical coherence tomography.

1. Introduction

Retinitis pigmentosa (RP) is a heterogeneous group of inherited human retinal diseases that cause degeneration of photoreceptors and the retinal pigment epithelium (Rattner, Sun and Nathans, 1999; Phelan and Bok, 2000). The genetic basis of the diseases is diverse, showing autosomal dominant (ad) and recessive, as well as X-linked recessive inheritance, and causal mutations have been documented in over 30 different genes (*http://www.sph.uth.tmc.edu/RetNet/*). There is also considerable variation in the pattern of disease in RP. Consistency of phenotype, however, has been demonstrated in molecularly defined subgroups of RP patients (e.g. Kemp et al., 1994; Jacobson et al., 1996a,b, 2000; Cideciyan et al., 1998).

We report an unusual RP disease pattern for which the gene defect is still unknown. This subgroup of patients has a centripetal loss of vision (from the far periphery toward the center). This is distinct from the pattern in most RP patients who show progressive retinal degeneration beginning in the mid peripheral or inferior retina. This uncommon topographic variant, which we term 'concentric RP', was recently described in a large study of visual field progression in RP (Grover, Fishman and Brown, 1998). To increase understanding of the pathogenesis and facilitate further gene discovery in retinal degenerative disease, new information is presented on the clinical features and histopathology of concentric RP.

2. Materials and Methods

Clinical Studies

The diagnosis of concentric RP was given to patients (Table I) with ophthalmoscopic evidence of

* Address correspondence to: Ann H. Milam, Scheie Eye Institute, University of Pennsylvania, 51 North 39th St. Philadelphia, PA 19104, U.S.A. E-mail: annmilam@mail.med.upenn.edu

0014-4835/01/100493+16 $35.00/0

TABLE I

Clinical characteristics of the patients

Patient no.	Age (years)*	Eye	Visual acuity**	Refraction†
Family of eye donor				
II-2	59	OD	20/25	−6·50
		OS	20/25	−6·25
II-3‡	74	OD	20/25	+9·25§
		OS	20/25	+8·75§
III-2	56	OD	20/40	+0·75
		OS	20/30	+0·50
III-3	56	OD	20/25	np
		OS	20/25	np
IV-2	16	OD	20/20	−2·75
		OS	20/20	−0·25
Other concentric RP patients				
1‖	30	OD	20/25	−8·00
		OS	20/25	−9·00
2‖	40	OD	20/400¶	−4·25
		OS	20/25	−4·25
3	28	OD	20/20	−3·75
		OS	20/20	−1·75
4	31	OD	20/30	−12·25
		OS	20/40	−12·75
5	36	OD	20/20	+0·50
		OS	20/20	plano
6	36	OD	20/30	−0·50
		OS	20/25	−0·50
7	51	OD	20/40	−5·00
		OS	20/30	−5·25
8	60	OD	20/25	+3·50§
		OS	20/25	+0·75§
9	69	OD	20/80	−5·75
		OS	20/60	−5·00

*At first visit or from record of ocular examination; **best corrected visual acuity; †spherical equivalent; ‡eye donor; §aphakic correction; ‖siblings; ¶macular hole; np, not performed.

retinal degeneration and the kinetic visual field pattern previously described (Grover et al., 1998). Specifically, patients were included who showed a relatively circular or slightly elongated Goldmann kinetic visual field with similar extents of field using V-4e and I-4e test targets. No patients had a history of taking vigabatrin (Wild et al. 1999). In the family of the eye donor, records from previous ocular examinations of the donor and other members were the source of most of the clinical and function test data. The daughter of the eye donor was the only family member examined in Philadelphia with the electroretinographic (ERG) and psychophysical methods. Unrelated simplex or multiplex patients with concentric RP ($n = 9$) or other forms of RP ($n = 11$) were also examined by us using kinetic perimetry, static threshold perimetry and ERGs. Cross-sectional retinal reflectivity profiles were obtained with optical coherence tomography (OCT; Humphrey Instruments, San Leandro, CA, U.S.A.) in one patient with concentric RP and a normal subject at the same superior retinal region. Details of the full field ERG, psychophysical (kinetic perimetry and dark and light adapted static perimetry), OCT methods and data analyses have been published (Jacobson et al., 1986, 1989, 1997, 1998, 2000; Cideciyan et al., 1998; Huang et al., 1998, 2000). Informed consent was given by all subjects and eye donors (see below). Institutional human subjects approval was obtained and the tenets of the Declaration of Helsinki were followed.

Genetic Diagnosis

DNA was extracted from peripheral blood and screened for coding sequence mutations in *rhodopsin* (*RHO*), peripherin/RDS and the Arg677ter mutation in *RP1*.

Histopathology

Post-mortem human eyes were obtained through the donor program of the Foundation Fighting Blindness (FFB, Owings Mills, MD, U.S.A.) and the University of Washington Lions Eye Bank. The eye from a 94 year old man (FFB #615) was fixed 17·5 hr post-mortem in a mixture of 4% paraformaldehyde and 0·5% glutaraldehyde in 0·1 M phosphate buffer, pH 7·3. After 3 weeks in this fixative, the globe was stored in 2% paraformaldehyde in the same buffer. As controls, normal eyes from two male donors (#0266-97, 82 year old, 1·5 hr post-mortem and #0164-00, 75 year old, 4·25 hr post-mortem) were processed in the same way.

Retinal samples were processed in glycol methacrylate, sectioned at 4 μm and stained with Richardson's mixture of methylene blue and azure II for light microscopy. Cryosections (12 μm) were stained with Oil Red O to reveal lipids. Control sections for the lipid stain were extracted with chloroform–methanol. Paraffin sections (5 μm) were stained with the following: Von Kossa method for calcium, Verhoeff–Van Gieson method for elastin (Newcomer Supply, Middleton, WI, U.S.A.), hematoxylin and eosin, and periodic acid Schiff (PAS) with or without hematoxylin.

As reported previously (Milam and Jacobson, 1990; Milam, 2000), retinal samples were treated with 1% sodium borohydride, infiltrated overnight at 4°C with 30% sucrose in 0·1 M phosphate buffer, pH 7·3, embedded in OCT (Miles, Inc., Elkhart, IN, U.S.A.), and cryosectioned at 12 μm. Sections were processed for immunofluorescence by published methods (Li, Kljavin and Milam, 1995a). The following retinal cell specific antibodies were used: mouse monoclonal antibody (mAb) 7G6 specific for cone cytoplasm and outer segments (1:250, from Dr P. MacLeish, Morehouse School of Medicine, Atlanta, GA, U.S.A.); mouse mAb 4D2 anti-rhodopsin specific for rod outer segments (1:40, from Dr R. Molday, University of British Columbia, Vancouver, B.C., Canada); rabbit pAb JH492 anti-red/green cone opsin (1:5000, from Dr J. Nathans, Johns Hopkins University, Baltimore, MD, U.S.A.); rabbit pAb anti-red/green cone opsin

(1 : 200, from Dr J. Saari, University of Washington, Seattle, WA, U.S.A.); rabbit pAb JH455 anti-blue cone opsin (1 : 5000, from Dr Nathans); rabbit polyclonal (pAb) anti-glial fibrillary acidic protein specific for astrocytes and reactive Müller cells (1 : 750, Dako Corporation, Carpinteria, CA, U.S.A.); rabbit pAb anti-laminin (1 : 100, Calbiochem, La Jolla, CA, U.S.A.); and biotinylated *Ricinus communis* agglutinin I (RCA) lectin (1 : 1000, Vector Laboratories, Burlingame, CA, U.S.A.) followed by rhodamine-avidin D (1 : 100, Vector Laboratories). The secondary antibodies (goat anti-rabbit or anti-mouse IgG, 1 : 50) were labelled with Alexa Fluor 488 (green; Molecular Probes, Eugene, OR, U.S.A.), Cy-2 (green), Cy-3 (red) or Cy-5 (blue) (Jackson ImmunoResearch Laboratories, Inc., West Grove, PA, U.S.A.). Cell nuclei were stained with 4′,6′-diamidino-2-phenylindole (DAPI, blue; 1 μg ml^{-1}; Molecular Probes) or Sytox (green; 1 μg per 300 ml; Molecular Probes). Control sections were treated in the same way with omission of primary antibody.

The immunolabelled retinal sections were examined with a microscope equipped for epifluorescence (Leica DMR, Deerfield, IL, U.S.A.) or with a laser scanning confocal microscope (BioRad MRC-600, Richmond, CA, U.S.A.). Images were digitized with a flat bed scanner (Saphir HiRes, Heidelberg CPS GmbH, Bad Hamburg, Germany) using LinoColor Elite 5.1 software (Heidelberg CPS GmbH), imported into a graphics program (Photoshop 5.0, Adobe, San Jose, CA, U.S.A.) and dye sublimation prints were generated.

3. Results

Eye Donor and Family Members: Clinical Studies

Five members of this family were known to have retinal degeneration [Fig. 1(A) and Table I]; male to male transmission and three generations with disease indicated ad inheritance. The clinical and psychophysical data from known affected members indicated intrafamilial consistency of the concentric RP disease expression.

Patient II-3, the eye donor died at age 94. He had a diagnosis of RP for at least 60 years before death. At age 90, visual acuities (VAs) were 20/25 and pigmentary retinopathy was present in the mid and far periphery but not in a wide extent of the central retina. Kinetic perimetry using various techniques over four decades showed a relatively circular residual field; the remaining central island was about 70–80° in diameter at age 40 and 40–50° at age 85.

Patient II-2, his sister, also had the diagnosis of RP. At age 59, VAs were 20/25 and there was

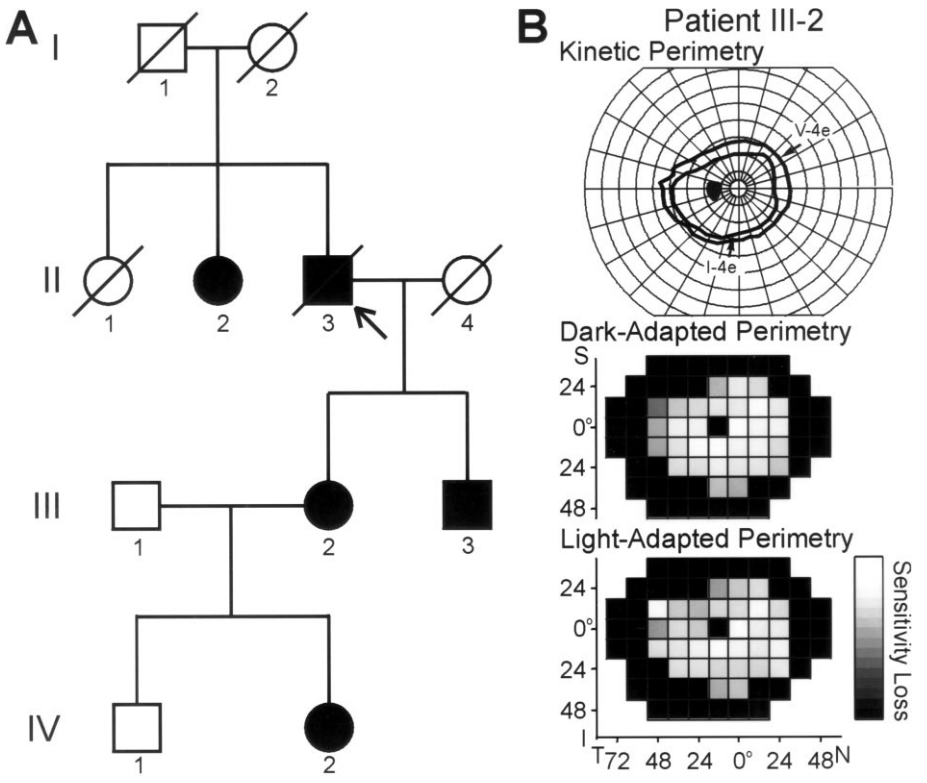

FIG. 1. Autosomal dominant concentric RP family of the eye donor. (A) Pedigree of this family with concentric visual field loss. (●), represent affected family members; (□), unaffected; (∅), deceased. Arrow indicates eye donor. (B) Kinetic perimetry (upper panel) with V-4e and I-4e targets from the left eye of the daughter (III-2, age 56) of the eye donor. Static threshold perimetry results in the dark adapted (middle) and light adapted (lower) states are displayed as grey scale maps of sensitivity loss. Scale has 16 levels of grey, representing 0 (white) to 6 (black) log units for dark adapted results and 0–3 log units for light adapted results. N, nasal; T, temporal; I, inferior; S, superior.

a relatively circular kinetic field about 60–70° in diameter. At age 88, after cataract surgery in both eyes, VA of the right eye remained 20/25 but the left eye had very reduced vision (cause unspecified).

Patient III-3, son of the donor, claimed no symptoms but carried the diagnosis of 'mild' RP since his mid forties. An examination at age 56 showed VAs of 20/25, small posterior subcapsular cataracts and peripheral pigmentary retinopathy.

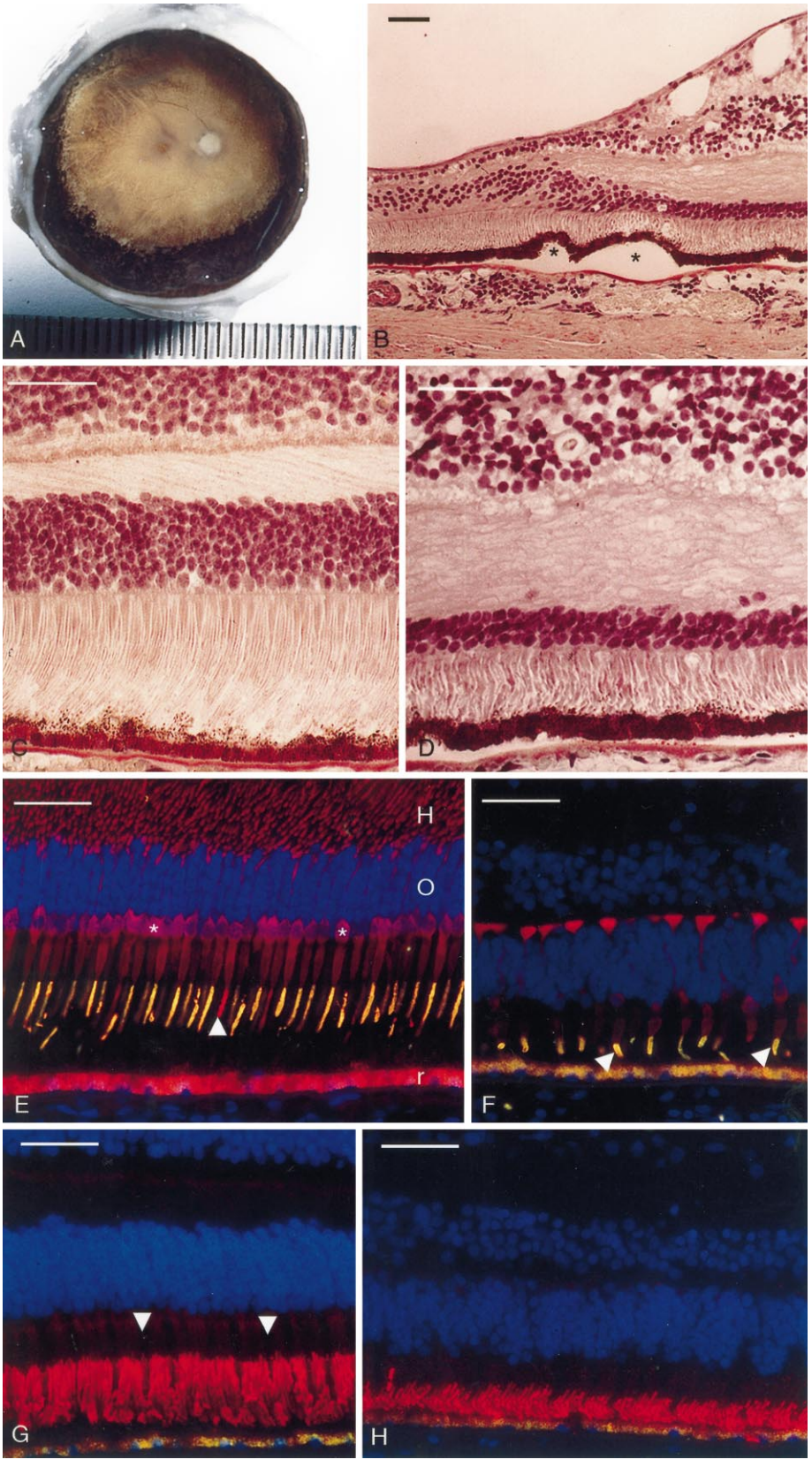

Patient III-2, daughter of the donor, was diagnosed with RP at age 30, although she was asymptomatic at that time. Visual field loss was noticed by the patient in her 40's and the presence of posterior subcapsular cataracts led to surgery in the left eye. Pigmentary retinopathy was noted throughout the peripheral retina; the central retina appeared normal and the retinal vessels were not attenuated. Rod and cone ERGs were reduced in amplitude and cone flicker timing was normal. Our examination of this patient at age 56 revealed VA in the right eye of 20/40 with a posterior subcapsular cataract; the pseudophakic left eye was 20/30. Kinetic perimetry of the left eye [Fig. 1(B), top panel] revealed a somewhat elliptical field extending from the 30° isopter nasally, inferiorly and superiorly and to 45° temporally. Visual field extent was abnormally reduced for both target sizes; a ratio of the extents (I-4e/V-4e) was 0·84. With dark adapted static threshold perimetry [Fig. 1(B), middle panel], the loci with detectable function were mainly rod mediated; rod sensitivity losses were < 1 log unit from mean. L/M cone function by light adapted increment thresholds [Fig. 1(B), lower panel] also showed some impairment and losses were < 1 log unit from mean. The rod ERG b-wave amplitude was reduced; a mixed cone–rod ERG had reduced a- and b-wave amplitudes; and cone flicker ERG amplitude was reduced but timing was normal [Fig. 8(C), open triangle, see below].

Patient IV-2, granddaughter of the donor, was diagnosed with 'atypical RP' at age 13. VAs were 20/25; peripheral pigmentary retinopathy was present. Kinetic perimetry showed a visual field to a large target with superior and inferior scotomas in the far temporal field. A smaller target revealed a relatively circular field of about 80–90° diameter [see Fig. 8(B) below]. At age 16, a definite demarcation was noted between the normal appearing central retina and the abnormal peripheral retina with pigmentary changes. Rod and cone ERGs were reduced in amplitude and cone flicker timing was normal. At age 24, VAs were 20/20 and a kinetic field was circular (about 80–90° diameter).

Genetic Diagnosis

Screening of three genes that can cause adRP, *RHO*, *peripherin/RDS*, and *RP1*, revealed no mutations in the coding sequences.

Eye Donor: Retinal Histopathology

Gross pathology. The eye was aphakic, with a peripheral iridectomy at 1200 hr. The anterior segment was otherwise normal for age. Some debris was present in the vitreous and the optic nerve head was pale and waxy. The retina contained heavy bone spicule pigment from the mid periphery to the ora serrata [Fig. 2(A)]. There was a sharp border between the bone spicule pigment and the more normal appearing central retina. The pigment was present in all four quadrants but was less dense in the superior nasal quadrant. The macula appeared thinned with some post-mortem edema.

Microscopic Pathology

Macula. The choroid and retinal pigment epithelium (RPE) appeared normal but the macula was thinned due to shortening of the rod and cone outer segments and irregular loss of some cells from the outer nuclear layer (ONL) [Fig. 2(B)]. The inner nuclear layer (INL) and ganglion cell layer (GCL) contained comparable numbers of cells in the normal and RP maculas. Compared with a normal fovea [Fig. 2(C)], the photoreceptors in the RP retina were decreased in number from 7–8 to 3–4 rows of nuclei and their outer segments were shortened from approximately 40 to 15 μm in length [Fig. 2(C) and (D)]. The macular cone outer segments were shortened to approximately 10–15 μm, as compared with normal macular cone outer segments which are approximately 30 μm in

FIG. 2. Observations on concentric RP and normal retinas used in study. Bars on all figures = 50 μm. (A) Gross pathology of eye. Note heavy bone spicule pigment from the ora serrata to the mid periphery. (B) Low magnification of fovea in RP retina. Two drusen (*) have been extracted during paraffin processing. Note some loss of photoreceptor nuclei and shortening of photoreceptor outer segments. Paraffin section, PAS and hematoxylin stain. (C) Macular photoreceptors in a normal retina. Note normal layers of photoreceptor nuclei and lengths of photoreceptor outer segments. Paraffin section, PAS and hematoxylin stain. (D) Macular photoreceptors in RP retina. Note decreased number of photoreceptor nuclei and shortened outer segments. Paraffin section, PAS and hematoxylin stain. (E) Macular cones in normal retina labelled with monoclonal antibody (mAb) 7G6 (red) and anti-red/green cone opsin (green). The cone cell bodies (*) form a row outermost in the outer nuclear layer (O). Most cone outer segments are double labelled (gold) with 7G6 and anti-red/green cone opsin. A single blue cone outer segment (arrowhead) is positive with 7G6 (red) but negative for red/green cone opsin. The retinal pigment epithelium (r) at the bottom of the panel contains autofluorescent lipofuscin granules. H, Henle fiber layer. Nuclei have been stained (blue) with DAPI. (F) Macular cones in RP retina labelled with mAb 7G6 (red) and anti-red/green cone opsin (green). Note reduced number of cones as compared with normal retina [Fig. 4(E)] and shortened cone outer segments (arrowheads). The RPE contains autofluorescent lipofuscin granules. Nuclei have been stained (blue) with DAPI. (G) Rods in normal macula labelled (red) with anti rhodopsin. Note negative images of cone inner segments (arrowheads). The RPE contains autofluorescent lipofuscin granules. Nuclei have been stained (blue) with DAPI. (H) Rods in RP macula labelled with anti-rhodopsin. Note shortened outer segments compared with the normal retina [Fig. 4(G)]. The RPE contains autofluorescent lipofuscin granules. Nuclei have been stained (blue) with DAPI.

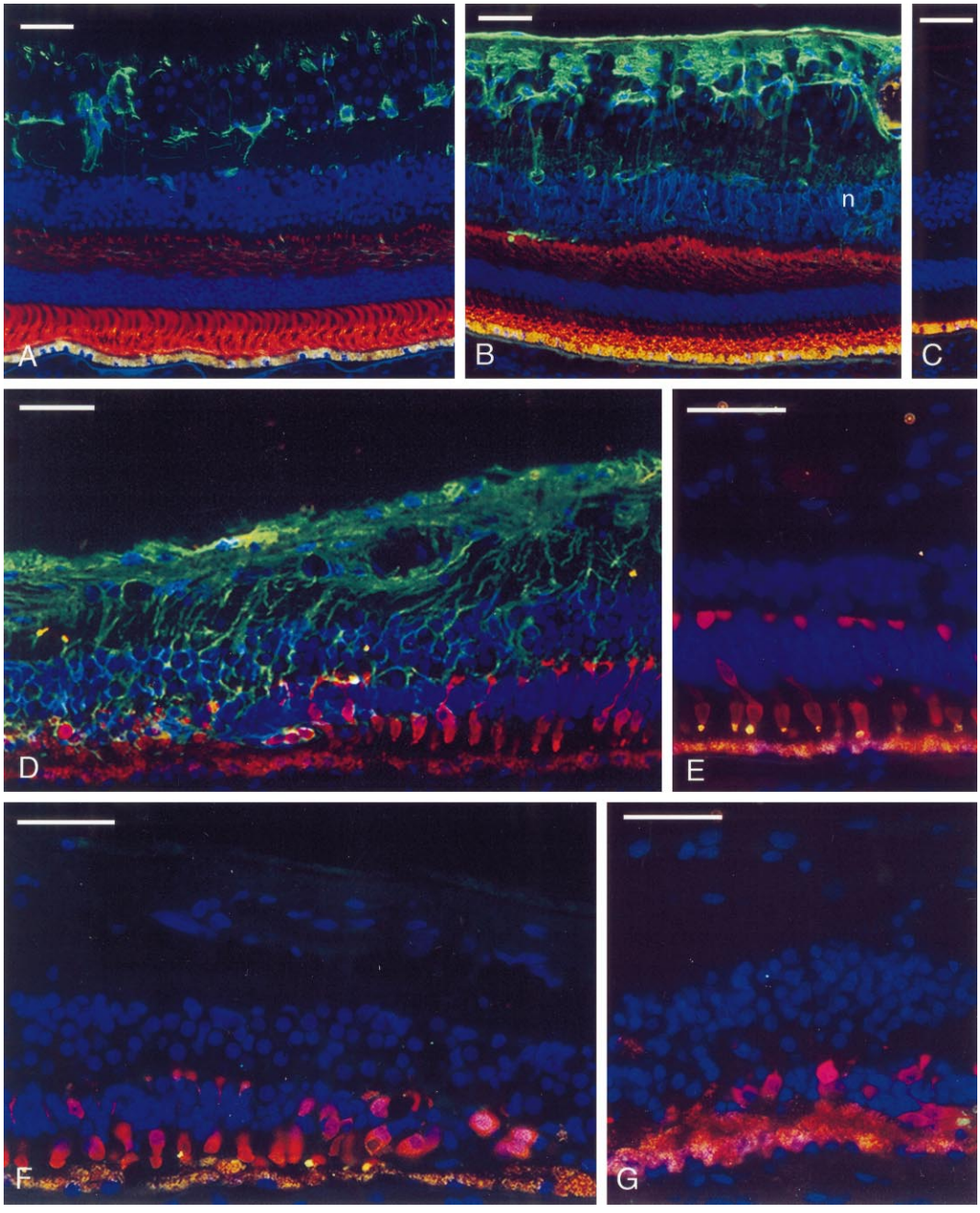

FIG. 3. Immunocytochemistry of concentric RP and normal retinas used in study. Bars on all figures = 50 μm. (A) Low magnification of macula of normal retina labelled with anti-GFAP (green) and anti-rhodopsin (red). GFAP immunoreactivity is restricted to astrocytes in the nerve fiber layer. The rhodopsin-positive rod outer segments are normal in length and the cone inner segments appear as negative images. The RPE contains autofluorescent lipofuscin granules. Nuclei have been stained (blue) with DAPI. (B) Low magnification of macula of RP retina labelled with anti-GFAP (green) and anti-rhodopsin (red). Note shortened rod outer segments and slightly increased GFAP in Müller cells in the inner nuclear layer (n), indicative that some cell death has occurred. The RPE contains autofluorescent lipofuscin granules. Nuclei have been stained (blue) with DAPI. (C) Control section of normal retina treated with no primary antibody but with Cy-2 and Cy-3 labelled secondary antibodies. Only the autofluorescent lipofuscin granules in the RPE are noted. Nuclei have been stained (blue) with DAPI. (D) Low magnification of zone of degeneration in the mid periphery of the RP retina labelled with mAb 7G6 (red) and anti GFAP (green). The more central cells are to the right; these cones show extreme shortening of their outer segments. Few photoreceptors remain in the more peripheral part (left) of the section. The RPE contains autofluorescent lipofuscin granules. Nuclei have been stained (blue) with DAPI. (E) Higher magnification of cones in zone of degeneration labelled with mAb 7G6 (red) and anti-red/green cone opsin (green). Note loss of cones and extreme shortening of their outer segments, which are double labelled (gold) with mAb 7G6 and anti-red/green cone opsin. The RPE contains autofluorescent lipofuscin granules. Nuclei have been stained (blue) with DAPI. (F) Degenerate cones labelled with mAb 7G6 (red) and anti-red/green cone opsin (green). A few stubby cone outer segments (gold) are retained. More degenerate cones lacking outer segments are toward the periphery (right). Nuclei have been stained (blue) with DAPI. (G) Degenerate cones lacking outer segments in the zone of degeneration. The cell bodies are positive (red) with 7G6 but only tiny cone outer segments (gold) remain, visualized by labelling with anti-red/green cone opsin. The RPE contains autofluorescent lipofuscin granules. Nuclei have been stained (blue) with DAPI.

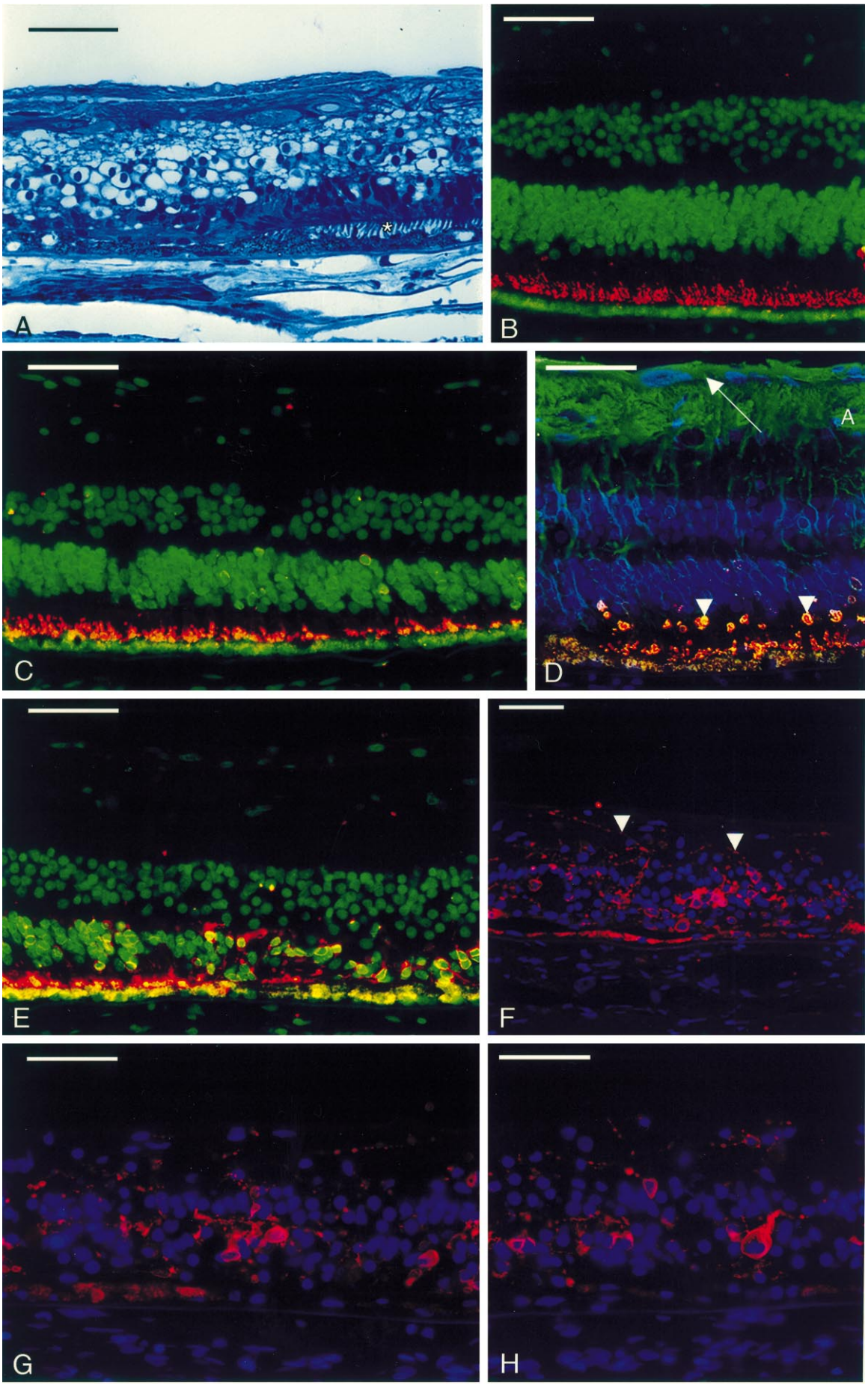

FIG. 4. Caption over page.

length [Fig. 2(E) and (F)]. Most of the cone outer segments were positive for red/green cone opsin [Fig. 2(E) and (F)] and a few were blue cone opsin-positive (not shown). The rods in the central retina were also slightly decreased in number and their outer segments were shortened from approximately 40 to 20 μm as compared with the control maculas [Fig. 2(G) and (H)].

In the normal retinas, GFAP reactivity was restricted to the astrocytes in the nerve fiber layer [Fig. 3(A)]. In the central region of the RP retina, secondary to loss of some photoreceptors, reactive Müller cells were weakly positive for GFAP, while astrocyte GFAP reactivity was normal [Fig. 3(B)]. Sections treated with no primary but with Cy-2 and Cy-3 labelled secondary antibodies showed only yellow-gold autofluorescence of lipofuscin granules in the RPE [Fig. 3(C)].

Mid periphery. This region spanned the interface between the bone spicule pigment and the more normal appearing central retina. On the central side of the interface, the RPE and retina showed near normal organization of layers [Fig. 3(D)], with four to six layers of INL cells and scattered ganglion cells. The ONL was irregular in thickness and in packing density of the nuclei, but had near normal numbers of cells (four to six rows of nuclei) on the central side of the interface. The cone outer segments central to the interface were shortened to 10 μm or less in length [Fig. 3(E)]. Within a narrow zone approximately 700 μm wide, the outer segments were lost from the photoreceptors and the ONL was markedly reduced [Fig. 3(F)]. Only a few cone somata lacking outer segments remained at this interface, and beyond this, cones were almost completely absent [Fig. 3(G)].

A similar pattern of cell loss was observed in the rods. The interface between more normal and severely degenerate retina was very sharp [Fig. 4(A)]. Central to this interface the rod outer segments were 15 μm or less in length [Fig. 4(B)] and next to the interface they were very short and stubby [Fig. 4(C)]. In the region bordering the interface, some rod inner segments contained clumps of rhodopsin-positive material and many rod somata showed delocalized labelling with anti-rhodopsin [Fig. 4(D)]. Müller cells adjacent to the interface were weakly GFAP-positive [Fig. 4(D)], consistent with ongoing photoreceptor cell death in the area.

As with the cones, the loss of rods was abrupt [Fig. 4(E)]. The few remaining rods in the interface zone lacked outer segments and had sprouted long, beaded neurites [Fig. 4(F), (G) and (H)]. A few rods, identified by their labelling with anti-rhodopsin, had markedly enlarged somata [Fig. 4(G) and (H)] up to approximately 20 μm in diameter.

Immediately peripheral to the zone of degeneration, the INL was reduced to one to three rows of nuclei and ganglion cells were absent. Müller cells were hypertrophied with enlarged nuclei that had migrated into the outer retina. More peripherally, the organized INL disappeared and retinal layering was completely lost. The nerve fiber layer was gliotic and a preretinal membrane [Figs 4(A), (D), and 5(A), (B)] of variable thickness (2–25 μm) contained spindle shaped cells positive for GFAP, which also filled the hypertrophied Müller cells. In the degenerate areas, numerous RPE cells had migrated into the retina, either as individual cells or as sheets of cells originating from Bruch's membrane [Fig. 5(B)]. The melanin granules in these RPE cells were round rather than oval as found in normal RPE cells, and migrated RPE cells had lost their lipofuscin granules. The RPE cells surrounded inner retinal blood vessels or were banked against the inner limiting membrane [Fig. 5(C)]. The RPE cells surrounded thick deposits of extracellular matrix (ECM), which occluded most of the retinal vessels. Some of the ECM deposits were not associated with RPE cells [Fig. 5(B)–(D)].

The ECM deposits were PAS- [Fig. 5(C)] and elastin-positive, stained pink by hematoxylin and eosin, and contained fine calcium spherules, stained black by the Von Kossa method [Fig. 5(D)]. Treatment of normal retinas and the central part of the RP retina with *Ricinus* lectin labelled drusen, rod outer segments, the inner limiting membrane, and vascular walls [Fig. 5(E)]. Like drusen, the ECM deposits in the

FIG. 4. Microscopy of concentric RP retina. Bars on all figures = 50 μm. (A) Plastic section of degeneration zone in mid periphery, showing retained photoreceptors with inner segments (*) to the right (central side of section). Richardson's methylene blue and azure II stain. (B) Rods near degeneration zone whose outer segments are labelled (red) with anti-rhodopsin. The RPE contains autofluorescent lipofuscin granules. Nuclei have been stained (green) with sytox. (C) Rods closer to the degeneration zone labelled with anti rhodopsin (red). Note extreme shortening of the rod outer segments toward the periphery (right side). The RPE contains autofluorescent lipofuscin granules. Nuclei have been stained (green) with sytox. (D) Rods very near the degeneration zone with inner segment deposits (arrowheads) of rhodopsin, labelled (red) with anti-rhodopsin. A preretinal membrane (arrow), astrocytes in the nerve fiber layer (A), and Müller cells in the inner nuclear layer are positive for GFAP (green). The RPE contains autofluorescent lipofuscin granules. Nuclei have been stained (blue) with DAPI. (E) Interface between more central rods with short outer segments labelled with anti-rhodopsin (red) to the left, and more peripheral degenerate rods lacking outer segments to the right. The RPE contains autofluorescent lipofuscin granules. Nuclei have been stained (green) with sytox. (F) Rods in the degeneration zone show cell body labelling with anti-rhodopsin (red) and have sprouted extensive neurites (arrowheads). The RPE contains autofluorescent lipofuscin granules. Nuclei have been stained blue with DAPI. (G) Higher magnification of enlarged rod cell bodies with neurites labelled with anti-rhodopsin (red) in the degeneration zone. Nuclei have been stained blue with DAPI. (H) Higher magnification of an enlarged rod cell body labelled with anti rhodopsin (red). Nuclei have been stained blue with DAPI.

concentric RP retina were positive by *Ricinus* labelling [Fig. 5(F)]. Treatment of normal retinas and the central part of the RP retina with anti-laminin labelled the basal laminae of the RPE cells, blood vessels and the inner limiting membrane [Fig. 6(A)]. In the concentric RP retina, the basal laminae surrounding the ECM deposits were positive with anti-laminin [Fig. 6(B)].

The ECM deposits were also positive by Oil Red O staining [Fig. 6(C) and (D)]. Within the deposits, fine granules of lipid could be resolved [Fig. 6(D)]. In addition to the RPE associated deposits, Bruch's membrane was positive for lipid [Fig. 6(C)–(F)]. Interestingly, Oil Red O-positive lipid droplets were also present in the inner segments of photoreceptors

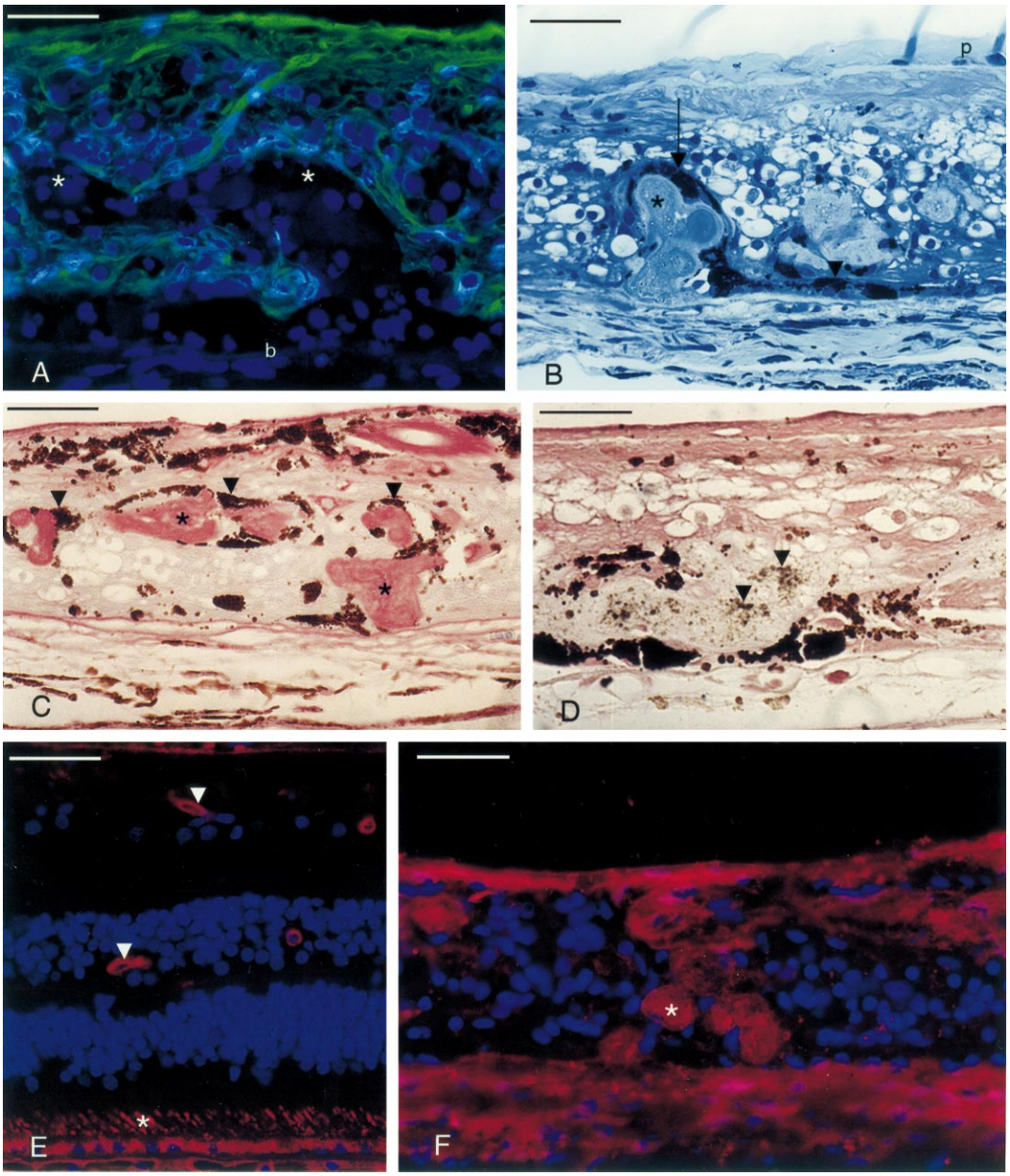

FIG. 5. Microscopy of periphery of the concentric RP retina. Bars on all figures = 50 μm. (A) Area of bone spicule pigment in far periphery of RP retina labelled with anti-GFAP. Note strong reactivity for GFAP (green) in Müller cell processes throughout the retina. The bone spicule pigment (*) extends as a sheet from Bruch's membrane (b) into the inner retina. Nuclei have been stained blue with DAPI. (B) Plastic section of bone spicule pigment stained with Richardson's methylene blue and azure II. Note sheet of pigmented RPE cells (arrow) that is continuous with RPE cells still in situ on Bruch's membrane (arrowhead). Deposits of extracellular matrix (*) are associated with the migrated RPE cells. Preretinal membrane, (p). (C) Paraffin section of far periphery of RP retina stained with PAS. Note deposits (*) of PAS-positive ECM associated with the migrated RPE cells (arrowheads). (D) Von Kossa stain of calcium spherules (black dots, arrowheads) in the extracellular matrix deposits in the far periphery of the RP retina. Eosin counterstain. (E) A more normal central part of the RP retina labelled with *Ricinus* lectin (red). Note staining of retinal blood vessels (arrowheads) and short rod outer segments (*). The RPE across the bottom of the plate contains autofluorescent (red) lipofuscin granules. Nuclei are stained (blue) with DAPI. (F) Far periphery of RP retina in area of bone spicule pigment. The extracellular matrix deposits (*) are strongly positive with *Ricinus* lectin. Nuclei are stained (blue) with DAPI.

central to the zone of abrupt rod and cone cell dropout [Fig. 6(E) and (F)]. These droplets were slightly smaller than the photoreceptor nuclei and were found only in photoreceptors adjacent to the zone of degeneration, and not in the photoreceptors in the central retina. Control sections for Oil Red O staining that had been extracted with chloroform–methanol were completely negative (not shown).

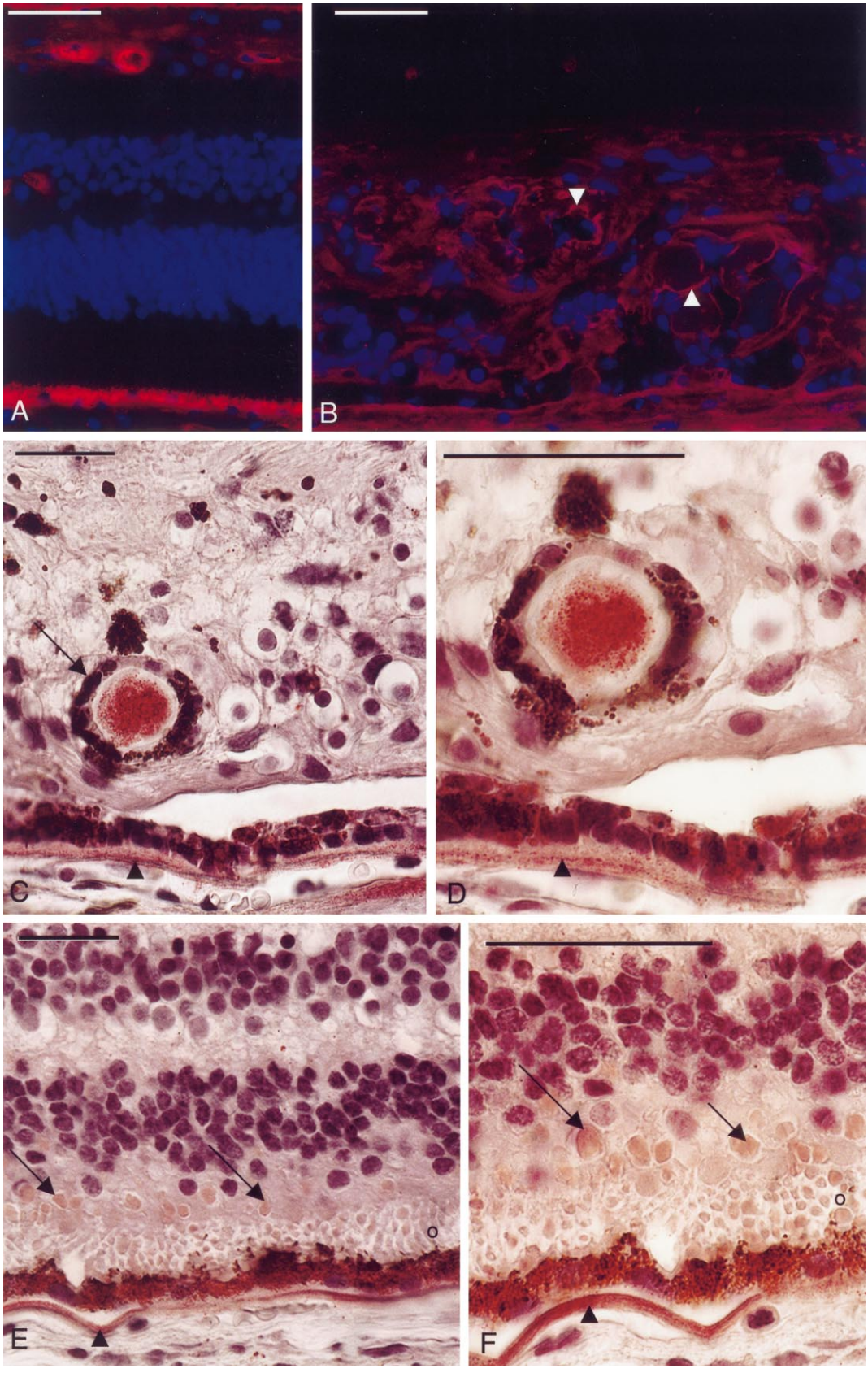

Far periphery. This region was completely degenerate with no photoreceptors. The retina was very thin and disorganized with marked gliosis. Only a few RPE cells remained in position against Bruch's membrane. Numerous intraretinal ECM deposits were present, not all surrounded by migrated RPE cells. In some cases, the ECM deposits originated from Bruch's membrane and extended intraretinally for several millimeters, surrounded in some areas by the migrated RPE cells. The INL was disorganized and gliotic and ganglion cells were absent. Most retinal vessels were occluded by ECM deposits.

Other Concentric RP Patients: Clinical and Visual Function Studies

A concentric pattern of visual field loss was also found in nine simplex or multiplex patients (five female, four male), representing eight different families; there were two siblings from one family [Patients 1 and 2, Table I]. Ages at first visit ranged from 30 to 69 years. All but the oldest had good VA (20/40 or better) and most were myopic. Fig. 7 illustrates the ophthalmoscopic appearance in three patients (A) and a cross-sectional retinal reflectivity image using OCT in another patient (B and C). Fundus photographs of the nasal and superior retina of Patient 3 show a relatively abrupt transition from healthy appearing central retina to pigmentary retinopathy. Views of the superior retina in siblings Patients 1 and 2 also show central retina with a relatively normal appearance and heavy pigmentary retinopathy in the peripheral retina with a less pigmented posterior edge. OCT in Patient 5 demonstrates that the ophthalmoscopically visible transition to pigmentary retinopathy is accompanied by a dramatic decrease in retinal thickness [Fig. 7(B) and (C)]. Scans in this patient that cross the zone from normal-appearing retina to pigmentary retinopathy and the graphical representation of the images indicate there is about 40–50 % reduction of thickness in the patient compared with about 10 % change over the same region in a normal subject.

Fig. 8 illustrates the typical kinetic perimetry result of concentric RP in three unrelated patients of different ages [Fig. 8(A)] and also proposes a sequence of kinetic field loss based on early and later stage data in three other patients [Fig. 8(B)]. Patients 9, 8 and 4, despite differences in age, have a similar pattern of visual field. The fields are relatively circular or slightly elongated (horizontally) and there are similar extents of the two targets. This feature of closely related dimensions of the kinetic visual field using the V-4e and I-4e test targets was quantified in these patients and compared with a series of simplex or multiplex patients with other forms of molecularly undefined RP ($n = 11$). The ratio of visual field extents, I-4e/V-4e, in the concentric RP patients had a mean value of 0·87 (S.D., 0·11) while the ratio in patients with other forms of RP showed a mean of 0·05 (S.D., 0·07). Statistical comparison of the two groups showed that the difference was significant ($P = < 0{\cdot}001$).

The circular pattern of visual field in these patients must be a disease stage that is preceded by loss of vision in the temporal field. Data from three patients suggest this proposed disease sequence. Patient IV-2, from the ad concentric RP family of the eye donor, had a kinetic field to the larger target with superior and inferior absolute scotomas that appear to be isolating a far temporal peripheral island of function from an extensive circular central island (defined with the smaller target). In Patient 3 at age 28, far peripheral temporal field islands were detectable with the large target and the circular central island had similar extents of the two targets; the peripheral islands were not detectable on a subsequent visit at age 32. Patient 2 may represent a late stage of disease with an irregular central island but similar extents of field with both target sizes. His younger sibling (Patient 1) had a larger extent of field and the same close relationship between field extents with the different targets.

Fig. 8(C) summarizes results of standard full field ERGs in one eye of the nine patients (●). Amplitudes for the responses displayed (rod b-wave to a dim blue flash in the dark adapted state, maximal white flash dark adapted, and light adapted cone ERGs to 1 Hz white flashes and 29 Hz flicker on a background) are subnormal (rectangles, ± 2 S.D., from the mean); cone flicker timing is within normal limits for all but two of the patients.

The topography of rod and cone mediated sensitivity losses in the visual field of simplex or multiplex patients ($n = 8$) with concentric RP further illustrate

FIG. 6. Microscopy of concentric RP retina. Bars on all figures = 50 μm. (A) More normal central part of the RP retina labelled with anti-laminin (red) reveals laminin surrounding the retinal blood vessels. The RPE across the bottom of the panel contains autofluorescent (red) lipofuscin granules. Nuclei are stained (blue) with DAPI. (B) Far periphery of RP retina shows labelling with anti-laminin (red) of the RPE basal laminae (arrowheads) around the deposits of extracellular matrix. The migrated RPE cells do not contain autofluorescent lipofuscin granules. Nuclei are stained (blue) with DAPI. (C) Far periphery of RP retina stained with Oil Red O and hematoxylin. The deposits of extracellular matrix associated with the migrated RPE cells (arrow) are strongly positive (red) for lipid. Bruch's membrane (arrowhead) also contains Oil Red O positive lipid. (D) Higher magnification of Fig. 8(C) showing Oil Red O labelling of ECM deposits. The Oil Red O positive material is finely granular in the deposits and in Bruch's membrane (arrowhead). (E) Mild peripheral area of the RP retina stained with Oil Red O and hematoxylin. Note Oil Red O positive droplets (arrows) in the inner segments of the photoreceptors, which have very short outer segments (o) and are near the zone of photoreceptor cell death. Bruch's membrane (arrowhead) is also Oil Red O positive. (F) Higher magnification of Oil Red O positive droplets (arrows) in the photoreceptor inner segments. The short outer segments (o) and Bruch's membrane (arrowhead) are also Oil Red O positive.

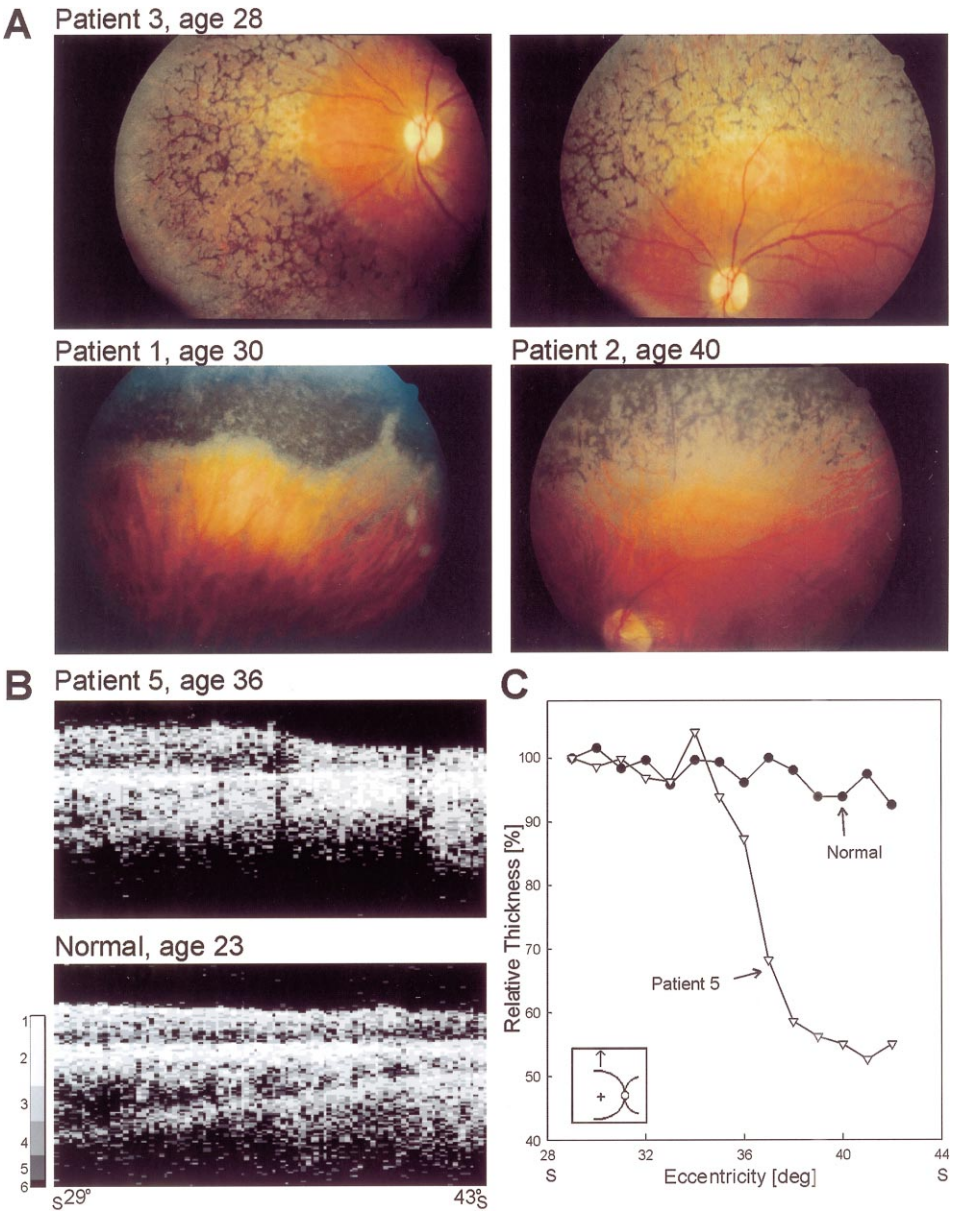

FIG. 7. Fundus photographs and OCT results in concentric RP patients illustrating the relatively abrupt transition from normal appearing retina to pigmentary retinopathy. (A) Fundus photographs of three simplex or multiplex patients with concentric RP. Upper panels: views of the left eye (left, nasal retina; right, superior retina) of Patient 3. Lower panels: superior retina views in two siblings, Patients 1 and 2. (B) Vertical OCT scans in the superior retinas of Patient 5 and a normal subject. For orientation, sclera is toward the bottom of the scans. OCT images are displayed with logarithm of reflectivity mapped to a grey scale; numbers 1–6 permit comparison to more commonly used pseudocolor displays (Jacobson et al., 2000). (C) Retinal thickness over the region of the transition zone in Patient 5 compared with a similar region in a normal subject. Scan depth was measured from the onset of the high vitread reflectivity (vitreoretinal interface) to the average peak of the more sclerad reflectivity (outer retinal choroidal complex) following alignment. Locations were identified by computer algorithm (Huang et al., 1998, 2000). To enable comparison of normal and patient data, scan depths were equated at 29° and relative thickness (%) plotted across the retinal region. Data points are averaged depth measurements over 1°.

the concentric pattern [Fig. 9(A)]. Measurements were made using dark and light adapted static threshold perimetry and color transitions depict the 50th percentile contour for a given level of sensitivity loss as specified on the color scale (Cideciyan et al., 1998; Jacobson et al., 2000). Fig. 9(B) shows horizontal profiles of dark adapted sensitivity to a 500 nm stimulus (left column) and light adapted sensitivity to a 600 nm stimulus (right column) in Patients 1,3 and 5. The profiles indicate that there can be normal or nearly normal function within the residual field despite differences in extent.

Screening for mutations in genes known to cause ad RP revealed no coding sequence changes in this group of other concentric RP patients.

4. Discussion

The concentric form of RP is a rare but recognizable topographical pattern of retinal degeneration (Grover

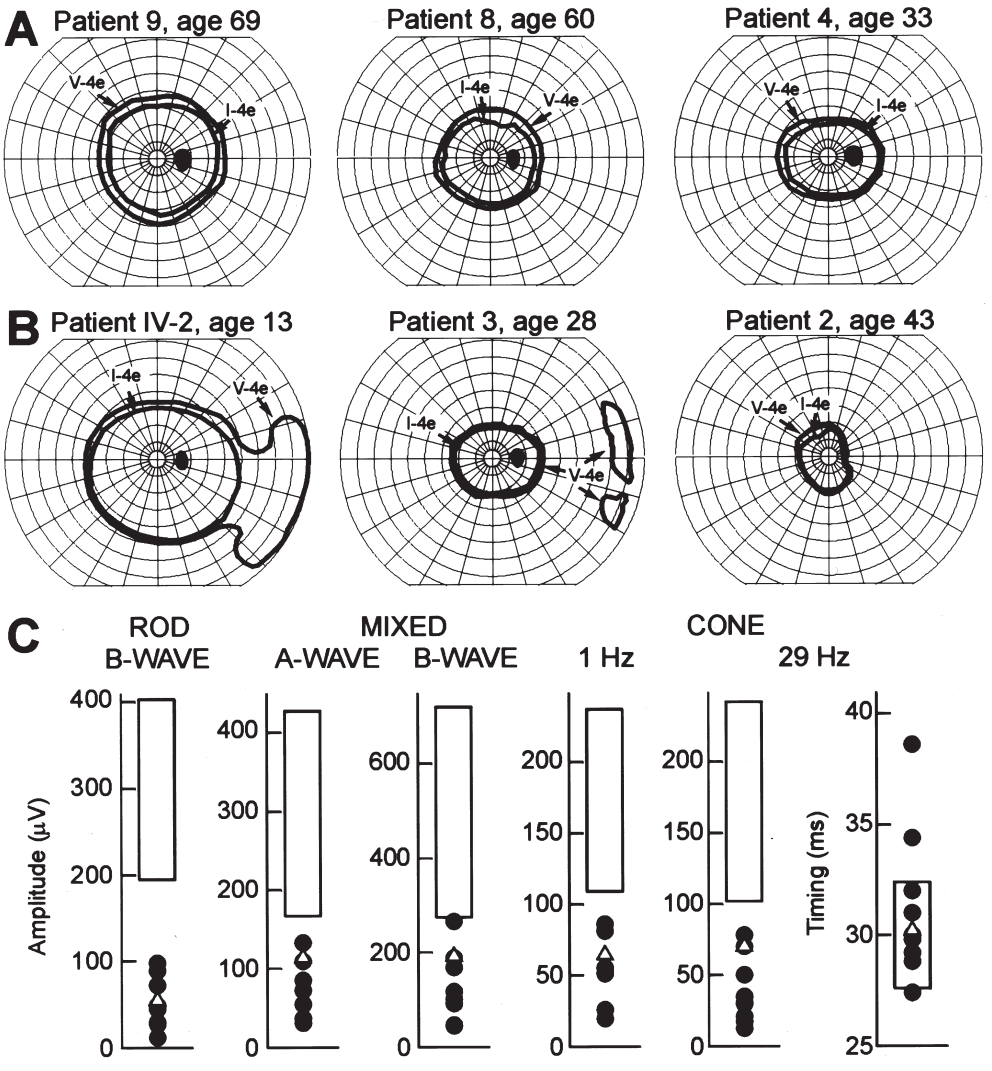

FIG. 8. Kinetic perimetry and ERGs in concentric RP. (A) Kinetic visual fields using V-4e and I-4e test targets in three simplex or multiplex patients, demonstrating similarity of field pattern. (B) Kinetic fields from three other patients (including Patient IV-2 from the eye donor's family) illustrating a proposed disease sequence based on these cross-sectional data. (C) ERG parameters from recordings in simplex or multiplex patients (●) and Patient III-2 from the family of the eye donor (△). Rectangles represent ± 2 S.D., from mean normal.

et al., 1998). The defining stage of the disease is when there is a wide, almost circular expanse of retina (centered at the fovea) that is normal or nearly normal in ophthalmoscopic appearance and in rod and cone function. This relatively normal retina is well demarcated from more peripheral retina that has pigmentary degeneration and no measurable visual function. It is expected that there must be an earlier disease stage preceding the time of circular fields when the temporal field of vision is lost. This stage was demonstrated in some patients who had circular central fields and residual temporal islands. Later stages likely involve slow progression of retinal degeneration toward the fovea from the boundaries of the large central island. Presumably, although outside of our clinical experience, there may be even later stages when this pattern merges with others and becomes indistinguishable.

The patients with concentric RP in the current study would fall under Pattern IA in the seminal work that classified patterns of visual field loss in RP (Grover et al., 1998). The patients probably represent a smaller subset of this group because of the additional restrictive criteria applied. Could the concentric pattern simply be a stage through which most RP patients pass on the way to a small central island of vision? The close relationship of isopters to the two conventionally used kinetic perimetric targets and near normal rod and cone mediated static perimetric thresholds within the boundaries of the residual field, together with the ophthalmoscopic signs of an abrupt transition from normal to degenerate retina, are not seen in other geographic patterns of RP, at least those that we have analysed with similar techniques (Cideciyan et al., 1998; Jacobson et al., 2000). The concentric geographic

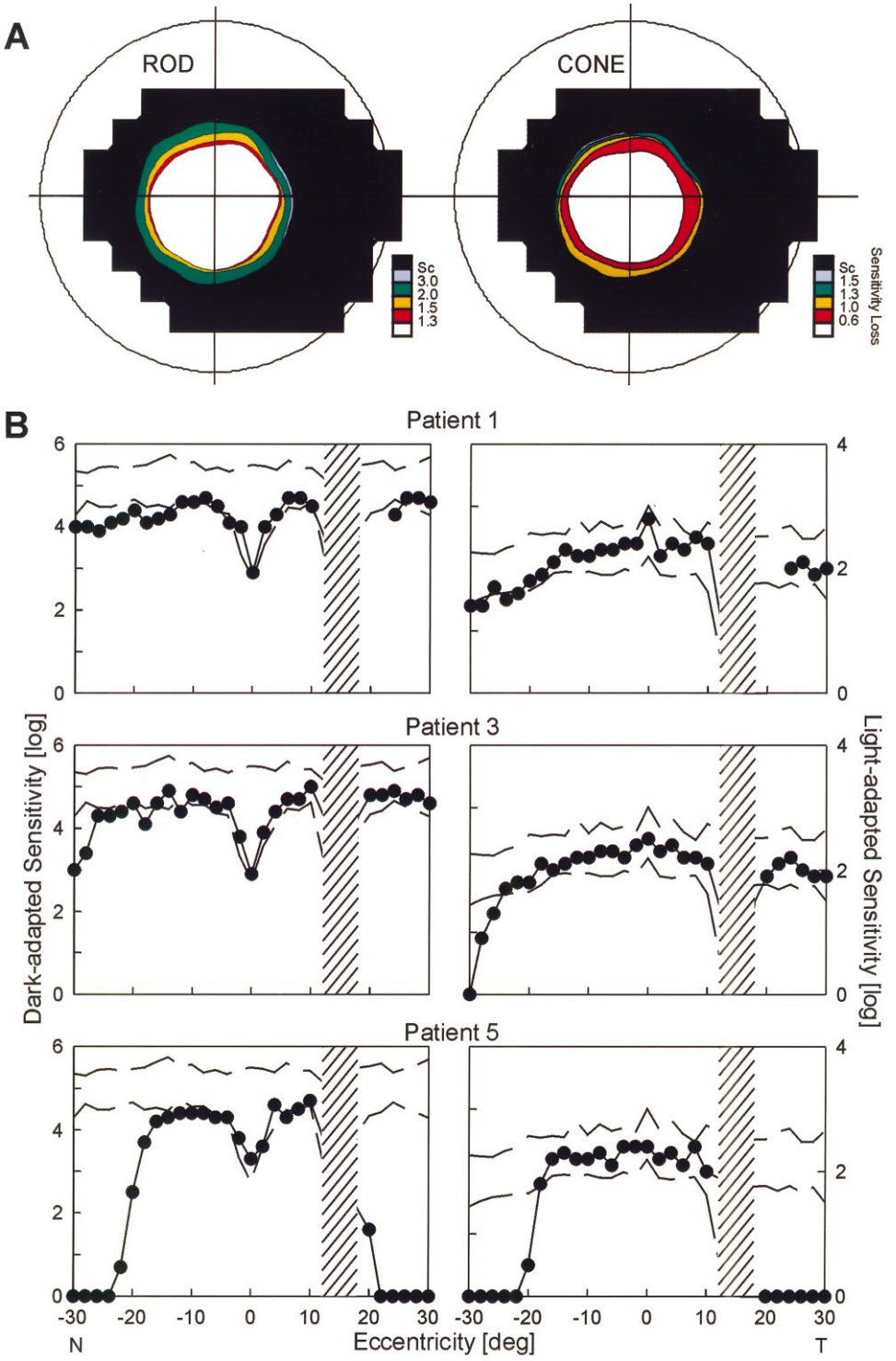

FIG. 9. Dark and light adapted static perimetry in concentric RP. (A) Topography of rod sensitivity loss (ROD; measured with 500 nm stimulus, dark adapted) and L/M (long/middle wavelength) cone sensitivity loss (CONE; 600 nm stimulus, light adapted) for simplex or multiplex patients ($n = 8$) with concentric RP. Color transitions depict the 50th percentile contour for a given level of sensitivity loss (specified on color scale). Maps are shown as a visual field of the right eye. (B) Horizontal profiles of dark adapted sensitivity to a 500 nm stimulus (left column) and light adapted sensitivity to a 600 nm stimulus (right column) in three patients (Patient 1, age 39; Patient 3, age 30; Patient 6, age 40) illustrating normal or nearly normal sensitivities within different extents of field.

pattern showed intrafamilial consistency in our ad RP family and in a multiplex family, suggesting that it is a heritable disease pattern rather than an individual expression. Screening of genes known to cause ad RP did not detect mutations in our patients.

In the donor retina from the ad concentric RP family, the disease was retina-wide with shortening of rod and cone outer segments throughout, but extreme differences in severity of expression between the periphery and center. The macula of the donor retina

appeared slightly thinned grossly but otherwise normal. Microscopically there was some photoreceptor cell loss and shortening of the rod and cone outer segments. The mid periphery showed similar changes in the photoreceptors up to an abrupt transition point where photoreceptor cells lacked outer segments and then were lost.

The far periphery, with heavy bone spicule pigment observed grossly, contained no photoreceptors and the retina was severely degenerate and gliotic. Previous descriptions of bone spicule deposits noted thick ECM deposits associated with the migrated RPE cells (Li et al., 1995a,Li, Possin and Milam, 1995b). The ECM deposits in the present case were numerous and extremely thick, and resembled drusen in their content of lipid, calcium, elastin and PAS- and *Ricinus*-positive materials. As shown previously (Li et al., 1995a,b), the ECM deposits occluded the vascular lumina, correlating with the severe loss of inner retinal neurons noted in the far periphery.

Use of Oil Red O stain to characterize the ECM deposits revealed novel lipid droplets in the inner segments of the photoreceptors near the zone of photoreceptor dropout. These lipid droplets were smaller than the photoreceptor nuclei and may correlate with an early stage of photoreceptor cell death. Cells of the RPE have been noted to undergo lipoidal degeneration (Fine and Kwapien, 1978; Tso and Fine, 1979; Fine, 1981; El Baba et al., 1986). However, to our knowledge, cytoplasmic lipid droplets have not previously been described in degenerating human photoreceptors; it is unknown if these novel droplets are unique to concentric RP or also found in other forms of photoreceptor disease.

Although a great deal of information is now available about specific gene mutations that cause RP, little is known about the different geographic patterns of visual field loss. Certain patterns are consistently associated with specific gene mutations. For example, a subgroup of ad RP patients with *RHO* mutations shows an inferior-nasal to superior-temporal retinal gradient of disease expression (Heckenlively, Rodriguez and Daiger, 1991; Li, Jacobson and Milam, 1994; Gal et al., 1997; Cideciyan et al., 1998). Presumably all rods across the retina express the mutant RP allele, yet not all degenerate at the same rate, suggesting that other factors influence the topographic pattern of photoreceptor death. From transgenic mice carrying a *RHO* mutation, it is known that dim overhead light accelerates rod cell death in the inferior retina (Naash et al., 1996). The same may be true for human patients with severe disease of the inferior retina, thought to reflect increased light levels incident to that region from overhead illumination (Heckenlively et al., 1991; Li et al., 1994). Another form of ad RP caused by *RP1* mutations shows early defects in the nasal retina, more inferior than superior (Jacobson et al., 2000). In many forms of RP, the mid periphery in all quadrants is the first area to degenerate (Grover et al., 1998) but the physiologic basis for this common pattern remains unknown.

Concentric RP is another topographic variant that requires elucidation. The pattern suggests that unknown retinal molecule(s) with peripheral to central gradients of distribution may be defective or modify photoreceptor degeneration in RP. Although intraretinal gradients of various molecules are present during development and postnatally (van Ginkel et al., 1995; Marcus et al., 1996; McCaffery et al., 1999; Schulte et al., 1999; Grün et al., 2000; Mic et al., 2000; Suzuki et al., 2000), to the authors' knowledge none of these gradients match the pattern of photoreceptor death found in concentric RP. Rather, the opposite is true for the distribution of one known photoreceptor survival factor, basic fibroblast growth factor, which is highest in rods in the far periphery and lowest in rods in the macula (Li, Chang and Milam, 1997). Much remains to be learned about possible gradients of other photoreceptor survival factors within the human retina, as well as the basis of the different geographic patterns of photoreceptor degeneration in RP.

Acknowledgements

Supported by Foundation Fighting Blindness; Paul and Evanina Bell Mackall Foundation Trust; Macula Vision Research Foundation; Macular Disease Foundation; Chatlos Foundation; Eye and Ear Foundation of Pittsburgh, NIH Grants EY-06855, -13132, -05627 and -13365; F.M. Kirby Foundation, Inc., and Research to Prevent Blindness, Inc (RPB). SGJ is a Senior Scientific Investigator of RPB. The authors thank the scientists listed in the Materials and Methods section for providing antibodies; Dr Tomas Aleman and Dr Artur Cideciyan for critical advice; Daniel Marks, Leigh Gardner and Dr Jiancheng Huang for graphics and data analyses; and Gulraiz Malik and Jama Bouy for technical assistance.

References

Cideciyan, A. V., Hood, D. C., Huang, Y., Banin, E., Li, Z.-Y., Stone, E. M., Milam, A. H. and Jacobson, S. G. (1998). Disease sequence from mutant *rhodopsin* allele to rod and cone photoreceptor degeneration in man. *Proc. Natl. Acad. Sci. U.S.A.* **95**, 7103–8.

El Baba, F., Green, W. R., Fleischmann, J., Finkelstein, D. and de la Cruz, Z. C. (1986). Clinicopathologic correlation of lipidization and detachment of the retinal pigment epithelium. *Am. J. Ophthalmol.* **101**, 576–83.

Fine, B. S. (1981). Lipoidal degeneration of the retinal pigment epithelium. *Am. J. Ophthalmol.* **91**, 469–73.

Fine, B. S. and Kwapien, R. P. (1978). Pigment epithelial windows and drusen: an animal model. *Invest. Ophthalmol. Vis. Sci.* **17**, 1059–68.

Gal, A., Apfelstedt-Sylla, E., Janecke, A. R. and Zrenner, E. (1997). Rhodopsin mutations in inherited retinal dystrophies and dysfunctions. *Prog. Ret. Eye Res.* **16**, 51–79.

Grover, S., Fishman, G. A. and Brown, J. (1998). Patterns of visual field progression in patients with retinitis pigmentosa. *Ophthalmology* **105**, 1069–75.

Grün, F., Hirose, Y., Kawauchi, S., Ogura, T. and Umesono, K. (2000). Aldehyde dehydrogenase 6, a cytosolic retinaldehyde dehydrogenase prominently expressed in sensory neuroepithelia during development. *J. Biol. Chem.* **275**, 41210–8.

Heckenlively, J. R. (1988). *Retinitis Pigmentosa*. J.B. Lippincott Company: Philadelphia, PA, U.S.A.

Heckenlively, J. R., Rodriguez, J. A. and Daiger, S. P. (1991). Autosomal dominant sectoral retinitis pigmentosa. Two families with transversion mutation in codon 23 of rhodopsin. *Arch. Ophthalmol.* **109**, 84–91.

Huang, Y., Cideciyan, A. V., Aleman, T. S., Milam, A. H. and Jacobson, S. G. (2000). Optical coherence tomography (OCT) in rhodopsin mutant transgenic swine with retinal degeneration. *Exp. Eye Res.* **70**, 247–51.

Huang, Y., Cideciyan, A. V., Papastergiou, G. I., Banin, E., Semple-Rowland, S. L., Milam, A. H. and Jacobson, S. G. (1998). Relation of optical coherence tomography to microanatomy in normal and *rd* chickens. *Invest. Ophthalmol. Vis. Sci.* **39**, 2405–16.

Jacobson, S. G., Buraczynska, M., Milam, A. H., Chen, C., Järveläinen, M., Fujita, R., Wu, W., Huang, Y., Cideciyan, A. V. and Swaroop, A. (1997). Disease expression in X-linked retinitis pigmentosa caused by a putative null mutation in the *RPGR* gene. *Invest. Ophthalmol. Vis. Sci.* **38**, 1983–97.

Jacobson, S. G., Cideciyan, A. V., Huang, Y., Hanna, D. B., Freund, C. L., Affatigato, L., Carr, R. E., Zack, D. J., Stone, E. M. and McInnes, R. R. (1998). Retinal degenerations with truncation mutations in the cone-rod homeobox (*CRX*) gene. *Invest. Ophthalmol. Vis. Sci.* **39**, 2417–26.

Jacobson, S. G., Cideciyan, A. V., Iannaccone, A., Weleber, R. G., Fishman, G. A., Maguire, A. M., Affatigato, L. M., Bennett, J., Pierce, E. A., Danciger, M., Farber, D. B. and Stone, E. M. (2000). Disease expression of *RP1* mutations causing autosomal dominant retinitis pigmentosa. *Invest. Ophthalmol. Vis. Sci.* **41**, 1898–908.

Jacobson, S. G., Cideciyan, A. V., Kemp, C. M., Sheffield, V. C. and Stone, E. M. (1996a). Photoreceptor function in heterozygotes with insertion or deletion mutations in the *RDS* gene. *Invest. Ophthalmol. Vis. Sci.* **37**, 1662–74.

Jacobson, S. G., Cideciyan, A. V., Maguire, A. M., Bennett, J., Sheffield, V. C. and Stone, E. M. (1996b). Preferential rod and cone photoreceptor abnormalities in heterozygotes with point mutations in the *RDS* gene. *Exp. Eye Res.* **63**, 603–8.

Jacobson, S. G., Voigt, W. J., Parel, J.-M., Nghiem-Phu, L., Myers, S. W. and Patella, V. M. (1986). Automated light- and dark-adapted perimetry for evaluating retinitis pigmentosa. *Ophthalmology* **93**, 1604–11.

Jacobson, S. G., Yagasaki, K., Feuer, W. J. and Roman, A. (1989). Interocular asymmetry of visual function in heterozygotes of X-linked retinitis pigmentosa. *Exp. Eye Res.* **48**, 679–91.

Kemp, C. M., Jacobson, S. G., Cideciyan, A. V., Kimura, A. E., Sheffield, V. C. and Stone, E. M. (1994). *RDS* gene mutations causing retinitis pigmentosa or macular degeneration lead to the same abnormality in photoreceptor function. *Invest. Ophthalmol. Vis. Sci.* **35**, 3154–62.

Li, Z.-Y., Chang, J. H. and Milam, A. H. (1997). A gradient of basic fibroblast growth factor in rod photoreceptors in the normal human retina. *Vis. Neurosci.* **14**, 671–9.

Li, Z.-Y., Jacobson, S. G. and Milam, A. H. (1994). Autosomal dominant retinitis pigmentosa caused by the threonine-17-methionine rhodopsin mutation: retinal histopathology and immunocytochemistry. *Exp. Eye Res.* **58**, 397–408.

Li, Z.-Y., Kljavin, I. J. and Milam, A. H. (1995a). Rod photoreceptor neurite sprouting in retinitis pigmentosa. *J. Neurosci.* **15**, 5429–38.

Li, Z.-Y., Possin, D. E. and Milam, A. H. (1995b). Histopathology of bone spicule pigmentation in retinitis pigmentosa. *Ophthalmology* **102**, 805–16.

Marcus, R. C., Gale, N. W., Morrison, M. E., Mason, C. A. and Yancopoulos, G. D. (1996). *Eph* family receptors and their ligands distribute in opposing gradients in the developing mouse retina. *Dev. Biol.* **180**, 786–9.

McCaffery, P., Wagner, E., O'Neil, J., Petkovich, M. and Drager, U. C. (1999). Dorsal and ventral retinal territories defined by retinoic acid synthesis, breakdown and nuclear receptor expression. *Mech. Dev.* **82**, 119–30.

Mic, F. A., Molotkov, A., Fan, X., Cuenca, A. E. and Duester, G. (2000). RALDH3, a retinaldehyde dehydrogenase that generates retinoic acid, is expressed in the ventral retina, otic vesicle and olfactory pit during mouse development. *Mech. Dev.* **97**, 227–30.

Milam, A. H. (2000). Immunocytochemical studies of the retina. *Meth. Mol. Med.* **47**, 71–88.

Milam, A. H. and Jacobson, S. G. (1990). Photoreceptor rosettes with blue cone opsin immunoreactivity in retinitis pigmentosa. *Ophthalmology* **97**, 1620–31.

Milam, A. H., Li, Z.-Y. and Fariss, R. N. (1998). Histopathology of the human retina in retinitis pigmentosa. *Prog. Ret. Eye Res.* **17**, 175–205.

Naash, M. L., Peachey, N. S., Li, Z.-Y., Gryczan, C. C., Goto, Y., Blanks, J., Milam, A. H. and Ripps, H. (1996). Light-induced acceleration of photoreceptor degeneration in transgenic mice expressing mutant rhodopsin. *Invest. Ophthalmol. Vis. Sci.* **37**, 775–82.

Phelan, J. K. and Bok, D. (2000). A brief review of retinitis pigmentosa and the identified retinitis pigmentosa genes. *Mol. Vis.* **6**, 116–24.

Rattner, A., Sun, H. and Nathans, J. (1999). Molecular genetics of human retinal disease. *Ann. Rev. Genet.* **33**, 89–131.

Schulte, D., Furukawa, T., Peters, M. A., Kozak, C. A. and Cepko, C. L. (1999). Misexpression of the EMX-related homeobox genes *cVax* and *mVax2* ventralizes the retina and perturbs the retinotectal map. *Neuron* **24**, 541–53.

Suzuki, R., Shintani, T., Sakuta, H., Kato, A., Ohkawara, T., Osumi, N. and Noda, M. (2000). Identification of RALDH-3, a novel retinaldehyde dehydrogenase, expressed in the ventral region of the retina. *Mech. Dev.* **98**, 37–50.

Tso, M. O. and Fine, B. S. (1979). Repair and late degeneration of the primate foveola after injury by argon laser. *Invest. Ophthalmol. Vis. Sci.* **18**, 447–61.

Wild, J. M., Martinez, C., Reinshagen, G. and Harding, G. F. (1999). Characteristics of a unique visual field defect attributed to vigabatrin. *Epilepsia* **40**, 1784–94.